MRS Communications (2019), 9, 92–98
© Materials Research Society, 2019
doi:10.1557/mrc.2018.241

MRS Communications

Research Letter

Self-healing liquid-infused surfaces with high transparency for optical devices

Meiling Zhang, **Qi Liu**, **Jingyuan Liu**, **Jing Yu**, and **Jun Wang**, Key Laboratory of Superlight Material and Surface Technology, Ministry of Education, Harbin Engineering University, Harbin 150001, China; College of Materials Science and Chemical Engineering, Harbin Engineering University, Harbin 150001, China

Address all correspondence to Jun Wang at **zhqw1888@sohu.com**

(Received 28 October 2018; accepted 17 December 2018)

Abstract

The glass surfaces used for optical devices are necessary to have high transparency. Here we propose to take advantage of tube-like SiO_2 textures to trap lubricant liquid inside aiming to prepare novel slippery liquid-infused porous surfaces (SLIPS). As a consequence, SLIPS with high transparency were synthesized on glass substrate successfully. The capillary action of unique tubular structure induces the ion migration of adjacent Krytox 100, thus endowing SLIPS with the self-healing property. Moreover, the remarkable slip behavior enables these surfaces to possess the self-cleaning and anti-biofouling performances. The current work might provide a promising candidate for long-term transparent optical devices.

Introduction

Highly transparent optical devices such as smart windows, solar panels, and optoelectronic devices, are frequently exposed to different outdoor environments for a long time, inevitably staining their outer surfaces. The adhesion of contaminants including dust, wet snow and bird droppings, could reduce the transparency of glass substrate and affects the power generation efficiency of solar cells.[1,2] Therefore, the glass surfaces used for such devices are necessary to keep high transparency, self-repairing and self-cleaning properties at the same time. Inspired by natural non-wetting structures, particularly the "lotus effect",[3] the superhydrophobic microtextured surfaces based on the formation of a stable air–liquid interface have been developed,[4,5] in which the superhydrophobic surfaces (SHSs) possess the self-cleaning, anti-fouling, and hydrophobic advantages.[6–10] However, the SHS are currently facing several key issues plaguing their research and applications: (1) oil droplets on SHS undergoes a high contact angle hysteresis, preventing its slide from the surface,[11] (2) the difficult slide of oil droplets due to the high contact angle hysteresis, the lost self-healing ability when attacked by physical damage and, (3) the high cost.[12,13] In addition, superhydrophobicity requires the surface must have a certain structural roughness, while the roughness means the loss of light scattering. In order to meet both transparency and superhydrophobicity at the same time, precisely controlling the surface roughness is necessary. Because of the wavelength range of visible light is 400–750 nm, the surface roughness of the transparent film should be controlled sub-100 nm in scale,[14,15] which needs a higher requirement on preparation technology. Moreover, the water droplets will transfer from the Wenzel–Cassie to the Wenzel state when condense on the roughness surface, leading a failure of superhydrophobic effect.

To compensate the defects of superhydrophobic materials, Wong et al. reported a strategy to create a new type of non-wetting surfaces, namely slippery liquid-infused porous surfaces (SLIPS), which possess good optical transparency, excellent liquid-repellency properties and pressure stability.[16] Since then, a lot of researches on SLIPS have appeared.[17–20] If applied on the design of the water-body, it can greatly reduce the resistance of the water body during underwater operation. Meanwhile, the slippery effect can improve the corrosion resistance and biologic resistance of the water body. SLIPS exhibit great application prospects in the design and manufacture of water bodies such as ships and submarines. The scientific significance and potential application value of SLIPS are widely recognized. However, it is worth noting that the slippery properties of SLIPS originate from the lubricant layer. The beneficial functions of SLIPS will dead away when the oil film disappears. If maintaining long-term slippery behavior for a long time, the special properties of SLIPS will make a great application in many fields, such as microfluidic control chip liquid non-destructive transmission, fluid drag reduction technology, heat transfer technology, and sensing smart surface. And SLIPS also can reduce the dust pollution and other pollutants in the air. Therefore, as Rykaczewski et al. emphasized,[21] it is highly desired to optimize the surface structure of SLIPS, such locking the lubricant inside and reducing its loss of lubricant.

https://doi.org/10.1557/mrc.2018.241 Published online by Cambridge University Press

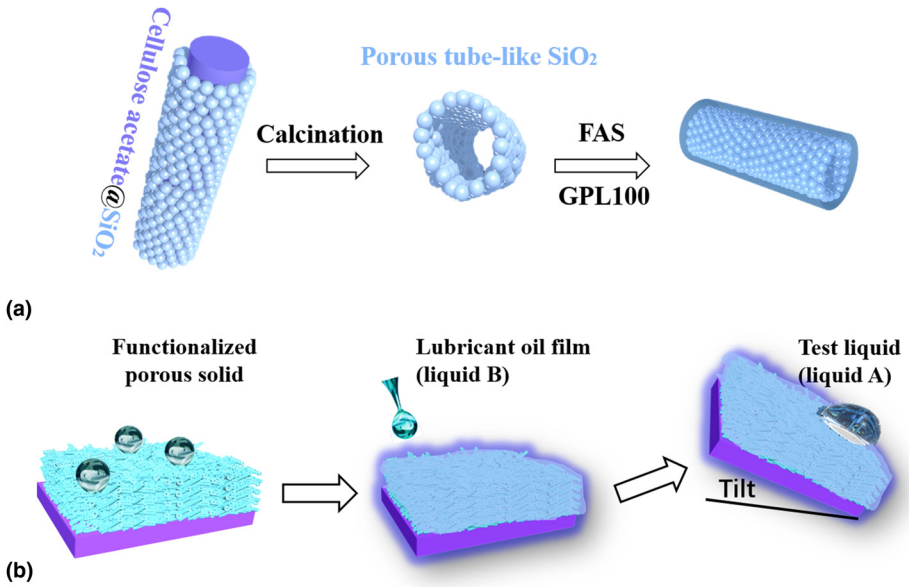


Figure 1. (a) The microscopic schematic illustration and (b) the macroscopic schematic illustration for the synthesis of SLIPS.

Herein, a silica tube composed of microsphere (about 50 nm) textures was prepared successfully. The tubular materials have a wall thickness of about 80 nm and an inner diameter of about 500 nm. Inspired by Lu et al.,[22] the glutaraldehyde (GA) was chosen as an adhesive to adhere the porous hollow tube-like SiO_2 to the glass substrate. And then the as-prepared sample was modified with (heptadecafluoro-1,1,2,2-tetradecyl)-trimethoxy silane (FAS), followed by pouring the lubricant oil into the surfaces to obtain a novel SLIPS. The as-prepared highly transparent slippery surfaces have remarkable slippery

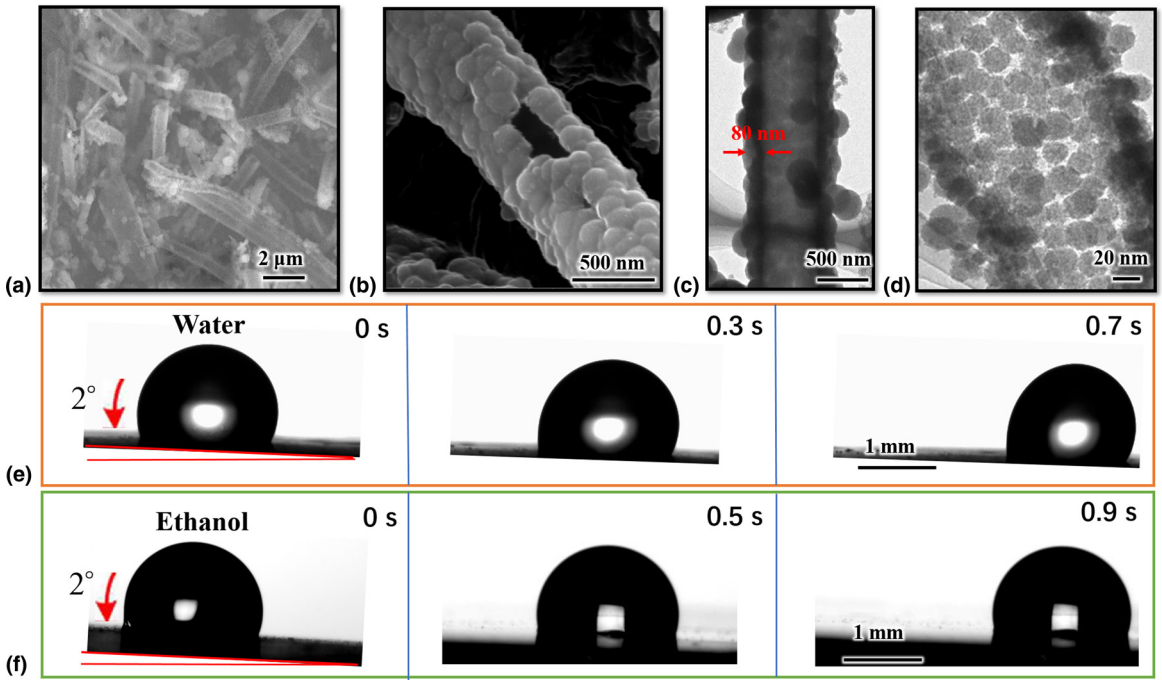


Figure 2. (a) Low-magnification and (b) high-magnification SEM images of hollow porous tubular SiO_2. (c) Low-magnification and (d) high-magnification TEM images of hollow porous tubular SiO_2 nanotube. (e) Water and (f) ethanol sliding behaviors on the SLIPS.

https://doi.org/10.1557/mrc.2018.241 Published online by Cambridge University Press

properties even standing for more than 45 days. It could be considered as a promising candidate for long-term transparent optical devices such as a windshield for automobiles, airplanes, spacecraft etc.

Experimental details

Materials

Cellulose acetate (CA), cetyltrimethylammonium bromide (CTAB, 99%), tetraethoxysilane (TEOS, 99.99%), FAS, and GA were purchased from Sigma-Aldrich. Microscope slides, acetone, and absolute ethanol were obtained from Aladdin Reagent Corp. (China). DuPont Krytox 100 lubricant (PFPE) was purchased from American DuPont Krytox.

Surface pretreatment of glass substrate

The glass slides were first washed with a wash solution (concentrated H_2SO_4:H_2O_2 = 3:1) until no more bubbles produced, and rinsed with deionized (DI) water. Then the treated slides placed in a dilute acid solution for 20 min, and rinsed with DI water, followed by the sonication in absolute ethanol for 20 min. Finally, the sonicated slides were rinsed with DI water and placed them in an oven for drying. The surface of the glass is enriched with a large number of hydroxyl groups.

Preparation of hollow porous tube-like SiO_2 (HPT-SiO_2)

HPT-SiO_2 was synthesized via an electrospinning method as reported in a previous paper.[23] Typically, CA fibers as templates were electrospun by a high-voltage electrospinning machine (TL-BM, 11 wt% CA acetone solution, voltage of 20 kV, distance of 15 cm, rate of 2 mL/h). 0.4 mL ammonia was dropped into the mixture solution containing 0.02 g CA, 0.027327 g CTAB, 45 mL DI water, and 10 mL ethanol, followed by ultrasonication for 30 min. And then 5 mL ethanol containing 160 µL TEOS was dropped into above solution and kept in 30°C for 2 h. Finally, CA@SiO_2 was transferred to the tube furnace, heated to 550°C at a rate of 3°C/min in an air atmosphere and maintained for 2 h. The CA template was removed and HPT-SiO_2 was obtained.

Preparation of SLIPS

0.2 g HPT-SiO_2 was placed in 20 mL of DI water, the solution pH was adjusted to 3 by acetic acid. And then 0.1 wt% KH550 was added to the solution under magnetic stirring for 20 min at room temperature, the surface of the HPT-SiO_2 after modified with KH550 has rich of amino groups. The treated glass was placed in the beaker and 1 mL 2.5% GA was added dropwise

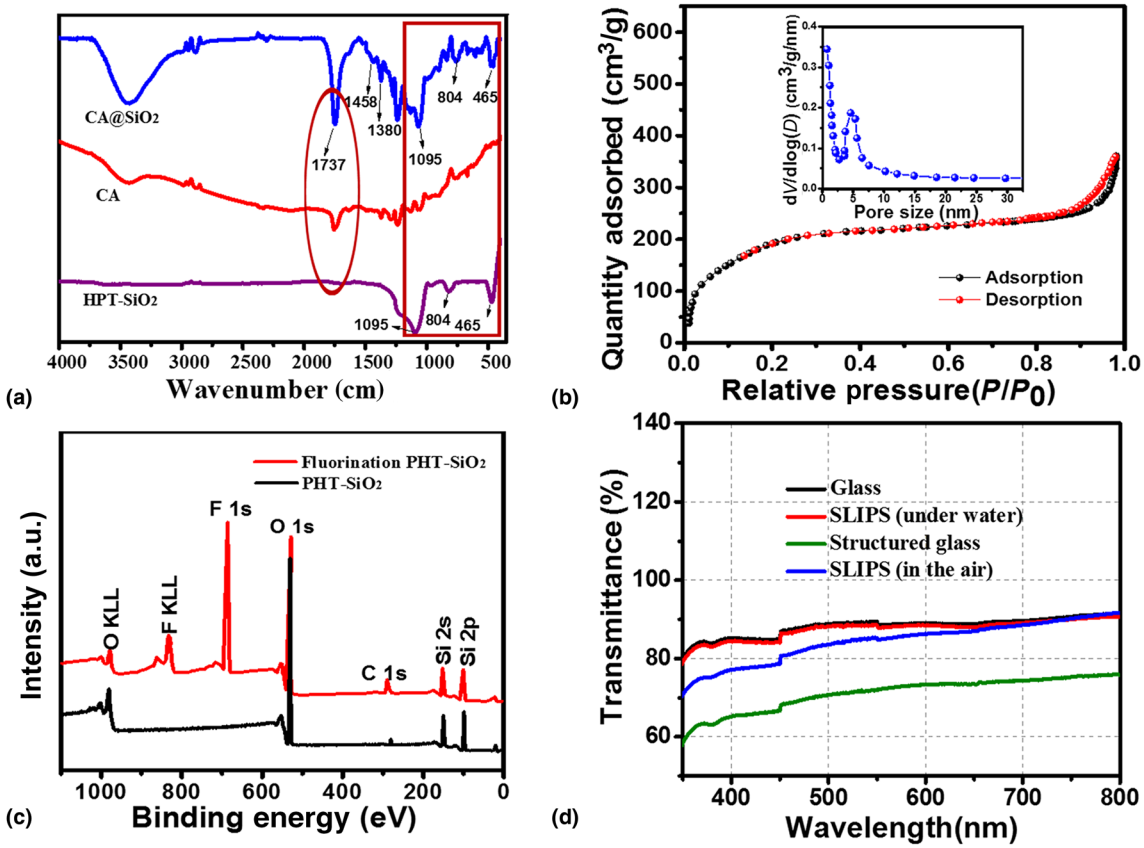


Figure 3. (a) The FTIR spectra of CA@SiO_2, CA, and HPT-SiO_2. (b) Nitrogen adsorption/desorption isotherm and pore size distributions of HPT-SiO_2. (c) XPS spectra of HPT-SiO_2 before and after modified by FAS. (d) Optical transmission measurements for difference surfaces in the 400–800 nm light range.

https://doi.org/10.1557/mrc.2018.241 Published online by Cambridge University Press

under stirring at 45°C and kept for 2 h to ensure the HPT-SiO_2 adhere to substrate firmly. In this process, one aldehyde group of GA reacts with a hydroxyl group on the glass and the other reacts with an amino group on HPT-SiO_2. The mixture of 0.1 g FAS and 9.9 g absolute ethanol was mechanically stirred for 2 h, and then the glass slide with HPT-SiO_2 was put into the above resulting solution for 2 h. The reaction mechanism is illustrated in Fig. S1. Followed by PFPE was dropped on the glass. Finally, the slide was placed vertically to drain excess oil to obtain SLIPS.

Characterization

The surface morphologies were determined by scanning electron microscopy (SEM) using a JEOL JSM-6480A at an accelerating voltage of 20 kV. Transmission electron microscopy (TEM) micrographs were characterized by a JEOL JEM 2100 microscope at a beam acceleration of 200 kV. Optical transmission measurements were carried out using an UV-Vis-NIR spectrophotometer. Static contact angles and slide angles were measured on a Data Physics OCA20 analysis system. The algae adhesion phenomenon was observed by an optical microscope (DFC 280). All digital photographs were taken by a Canon digital camera. To ensure the reproducibility, all of the measurements were repeated for at least three times.

Results and discussion

Figure 1(a) shows the microscopic schematic illustration for the synthesis of SLIPS. SiO_2 microspheres were adsorbed on the surface of CA fiber. After calcination, the hollow porous silica tubes were obtained. After FAS modification, the lubricant was poured into the tube to obtain a novel tubular SLIPS. As seen from Fig. 1(b), in order to match the chemical properties of the lubricant better, the low-surface-energy modifiers were grafted to the surfaces. The functionalized porous surface has superhydrophobic properties with the contact angle of 162°, indicating the successful fluorination (see Fig. S2). Then the substrate is preferentially wetted by the lubricant and finally the SLIPS have visible slippery properties of repelling complex liquid at a small tilt angle.

Figures 2(a) and 2(b) show the low and high-magnification SEM images of hollow porous tube-like SiO_2. After calcination, the CA fiber was completely removed but remained its

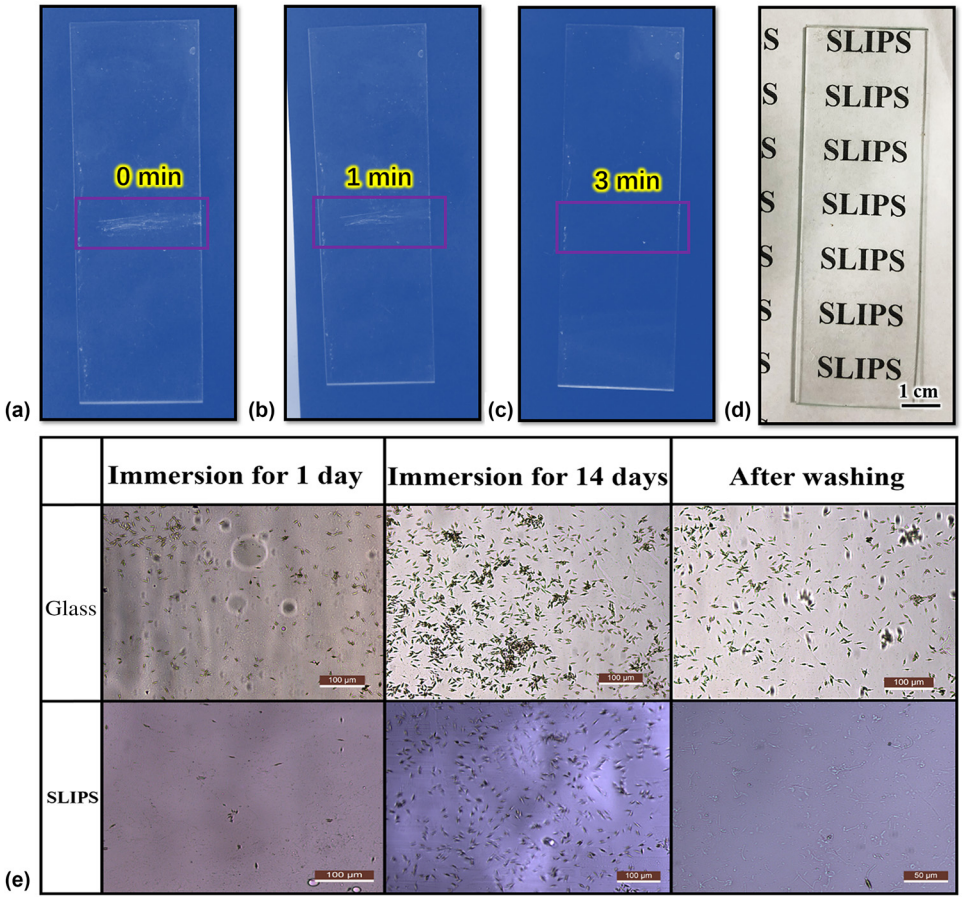


Figure 4. (a–d) Time sequence digital images showing the self-healing action. (e) The algae attachment images after 1 and 14 days soaking, as well as after being washed, of blank glass and SLIPS.

https://doi.org/10.1557/mrc.2018.241 Published online by Cambridge University Press

appearance. The production has been well formed into a tube. The TEM images further prove the hollow structure. The thickness of tube wall is about 80 nm and the tube diameter is about 500 nm [Fig. 2(c)], which provides good carrier for oil to obtain high transparency. The uniform porous tube benefits to lock the lubricant and the microporous structure of tube wall endows the coating with self-repairing properties by the capillary action. Once the oil layer on outmost surface was lost, the lubricant would penetrate from the microporous structure to the upper surface, making sure that there always has a lubricating layer on the upper surface. The presence of lubricating layer allows water or ethanol to float above the substrate. The droplets can slide off the glass easily at tilt 2° [Figs. 2(e) and 2(f), the sliding velocity is 2 mm/s], which endows the SLIPS with self-cleaning property.

The FTIR spectrum of CA@SiO_2 contains all the characteristic absorption peaks of silica and CA [Fig. 3(a)]. The peak at 1095/cm belongs to the antisymmetric stretching vibration of Si–O–Si. The two peaks located at 804 and 465/cm are assigned to the symmetric stretching vibration and the bending vibration of Si–O–Si, respectively. These results prove that silica is successfully adsorbed on the template. The FTIR spectrum of HPT-SiO_2 shows no absorption band at 1737/cm, indicating that the CA templates were completely removed. Figure 3(b) describes the N_2 adsorption/desorption isotherm and pore size distributions of HPT-SiO_2. The adsorption amount of N_2 increases sharply in $P/P_0 = 0.7–1.0$. The capillary action causes an irreversible phenomenon of adsorption and desorption, and hysteresis loop resembles the H4-type in the IUPAC classification.[24] The material has the characteristics of a microporous mesoporous molecular sieve. The BET surface area of HPT-SiO_2 is calculated to be 686.04 m^2/g. According to the BJH model, the diameter of the mesopores is about 5.7 nm, and the median pore width is 0.8 nm. In order to match the chemical properties of the lubricating oil, SiO_2 was fluorinated. The XPS survey spectra before and after fluorination are shown in Fig. 3(c). The only difference between the two curves is the content of F_{1s} and F_{KLL}, which proves that the successful fluorination. Optical transmission in the ultraviolet visible range for different surfaces is depicted in Fig. 3(d). The transmittance of bare glass is 91%, while the transmittance of glass after spraying (structured glass) is greatly reduced with the highest point of 78%. The decrease in light transmittance is caused by light scattering of composite particles in the coating. Lubricant infusion is beneficial to greatly

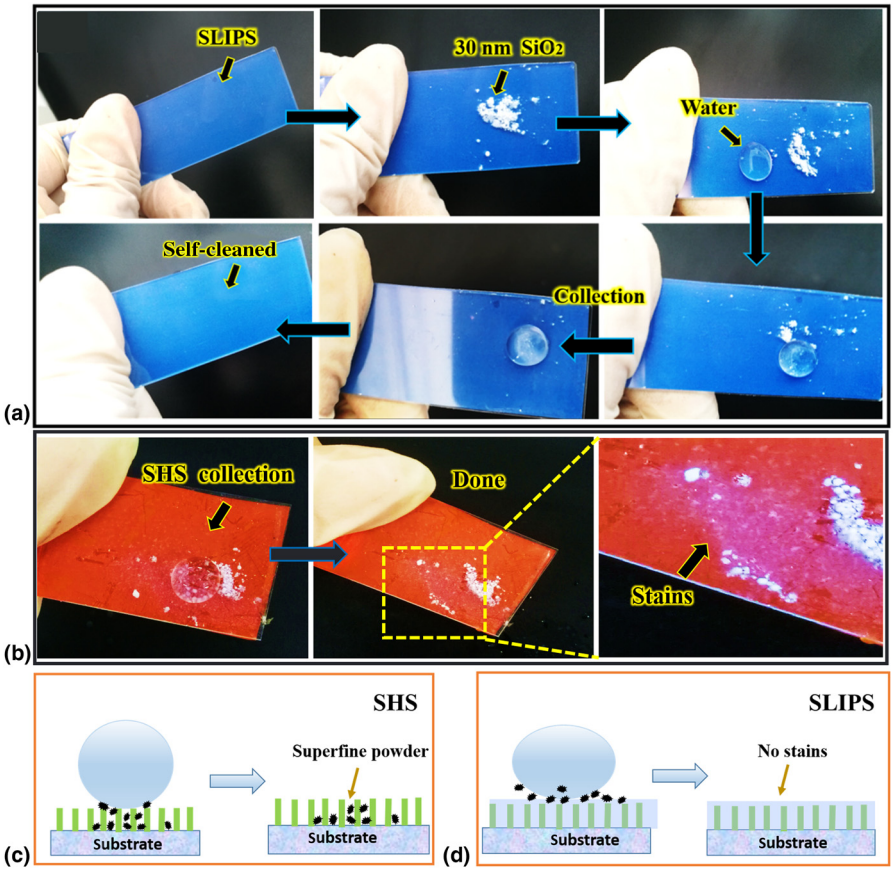


Figure 5. Digital images showing the subsequent self-cleaning action using a water droplet to clean hydrophilic SiO_2 powder (about 30 nm) on (a) SLIPS and (b) SHS. Schematic illustration of the self-cleaning way for (c) SHS and (d) SLIPS.

https://doi.org/10.1557/mrc.2018.241 Published online by Cambridge University Press

increase the transmission of SLIPS. The transparency increased to 90.8% underwater and increased to 89% in air. In other words, it can maintain high transparency in high humidity or rainy days, which can significantly improve enhance the visibility, thus improving driving safety. When used as high-rise building curtain walls, SLIPS could reduce the number of cleaning and avoid the danger of working at height. This also encourages the as-prepared SLIPS to apply to underwater optical devices such as sensors and cameras.

Figures 4(a)–4(d) depict self-repairing behavior of the as-prepared SLIPS. In the middle position of Fig. 4(a), there is a sandpaper wear mark (0.5×1.5 cm^2). Placed in a room temperature environment without any intervention for 1 min, the scratches became shorter and narrower [Fig. 4(b)]. After 3 min, the scratch mark disappeared completely [Fig. 4(c)]. The scratched area still maintains high transparency after repairing and the under pattern is clearly visible [Fig. 4(d)]. The self-healing behavior could be attributed to the synergistic interaction of ion migration of adjacent Krytox 100 and capillary effect of the tube structure.[25–27]

When using transparent SLIPS as underwater optical components, the anti-biofouling properties should be an important reference. Algae are one of the most common marine fouling organisms in the marine environment. Effective anti-attachment of algae will contribute to the practical application of SLIPS. To evaluate the anti-algae effect of the as-prepared SLIPS, the coating was immersion in algae liquid. After 1 day, bare glass and SLIPS present big difference, as illustrated in Fig. 4(e), large number of algae were found to attach on the glass surface, while only a few algae were found on the SLIPS. It is preliminarily deduced that algae prefer to adhere to a harder solid surface compared with a "soft surface". After 14 days immersion, the two surfaces are heavily covered with algae. Both of the two surfaces are accompanied by a layer of yellow-green algae liquid by the macroscopic observation. However, the algae are in a migratory state on the SLIPS surface by microscope observation. After further rinsing, we found that almost all the algae on the SLIPS were washed away but the glass still adhered to a large number of algae. These results proved that SLIPS can resist bio-adhesion effectively.

No matter in SHS or in SLIPS system, the self-cleaning behavior plays an important role in solving the environmental pollution and water waste caused by glass cleaning. As illustrated in Fig. 5(a), the superfine and hydrophilic SiO_2 on SLIPS can be collected and slide down easily. On the contrary, SHS allows water droplet to roll freely and to take away the relatively large dust. The superfine dust fills the air cushion of the SHS and cannot be carried away by water droplets. After processing the partially enlarged image (increasing the image saturation), white traces can be clearly seen [Fig. 5(b)]. When the superfine dust accumulates inside the structure, the three-phase contact line will be destroyed, resulting in superhydrophobic failure, and thus losing self-cleaning property [schematic in Fig. 5(c)]. Noteworthily, by filling the lubricant into the surface structure previously to form a SLIPS, the ultra-fine dust floats on the surface, and then the silica particles are wicked to the water droplets [schematic in Fig. 5(d)], thus accomplishing the self-cleaning process of SLIPS, which demonstrates the long-term potential for SLIPS in self-cleaning applications.

Conclusions

A novel and mechanical robust SLIPS with porous hollow tubular SiO_2 was synthesized on the glass substrate successfully. The prepared SLIPS exhibit a highly liquid repellency properties, as well as excellent self-cleaning and self-healing performances. The tube-like textures are responsible for the capillary action and storage capacity of lubricant which enables the slippery surfaces to maintain long-term outstanding slippery properties. The SLIPS possess good transmittance in air (89%) and underwater (90.8%) in visible range. These surfaces also show excellent anti-biofouling properties because of their slippery characteristic. Designed SLIPS provides attractive prospects for applications in anti-fouling, self-cleaning materials, and optical devices.

Acknowledgments

This work was supported by the National Natural Science Foundation of China (No. 51603053), the Application Technology Research and Development Plan of Heilongjiang Province (GX16A008), the Fundamental Research Funds of the Central University and the Application Technology Research and Development Projects of Harbin (2015RAQXJ038), Defense Industrial Technology Development Program (JCKY2016604C006) and National Key R&D Program of China (2016YFE0202700).

Supplementary material

The supplementary material for this article can be found at https://doi.org/10.1557/mrc.2018.241

References

1. L. Zhang, C.-H. Xue, M. Cao, M.-M. Zhang, M. Li, and J.-Z. Ma: Highly transparent fluorine-free superhydrophobic silica nanotube coatings. *Chem. Eng. J.* **320**, 244 (2017).
2. K. Golovin, D.H. Lee, J.M. Mabry, and A. Tuteja: Transparent, flexible, superomniphobic surfaces with ultra-low contact angle hysteresis. *Angew. Chem. Int. Ed.* **52**, 13007 (2013).
3. W. Barthlott and C. Neinhuis: Purity of the sacred lotus, or escape from contamination in biological surfaces. *Planta* **202**, 1 (1997).
4. P. Dimitrakellis and E. Gogolides: Hydrophobic and superhydrophobic surfaces fabricated using atmospheric pressure cold plasma technology: a review. *Adv. Colloid Interface Sci.* **254**, 1 (2018).
5. W. Wang, Y.-Q. Liu, Y. Liu, B. Han, H. Wang, D.-D. Han, J.-N. Wang, Y.-L. Zhang, and H.-B. Sun: Direct laser writing of superhydrophobic PDMs elastomers for controllable manipulation via Marangoni effect. *Adv. Funct. Mater.* **27**, 1702946 (2017).
6. X. Tang and L. Wang: Loss-free photo-manipulation of droplets by pyroelectro-trapping on superhydrophobic surfaces. *ACS Nano* **12**, 8994 (2018).
7. V. Jokinen, E. Kankuri, S. Hoshian, S. Franssila, and R.H.A. Ras: Superhydrophobic blood-repellent surfaces. *Adv. Mater.* **30**, 1705104 (2018).

https://doi.org/10.1557/mrc.2018.241 Published online by Cambridge University Press

8. L. Feng, S. Li, Y. Li, H. Li, L. Zhang, J. Zhai, Y. Song, B. Liu, L. Jiang, and D. Zhu: Super-hydrophobic surfaces: from natural to artificial. *Adv. Mater.* **14**, 1857 (2002).
9. X. Tian, S. Shaw, K.R. Lind, and L. Cademartiri: Thermal processing of silicones for green, scalable, and healable superhydrophobic coatings. *Adv. Mater.* **28**, 3677 (2016).
10. G.B. Hwang, K. Page, A. Patir, S.P. Nair, E. Allan, and I.P. Parkin: The anti-biofouling properties of superhydrophobic surfaces are short-lived. *ACS Nano* **12**, 6050 (2018).
11. L. Bocquet and E. Lauga: A smooth future? *Nat. Mater.* **10**, 334 (2011).
12. R. Poetes, K. Holtzmann, K. Franze, and U. Steiner: Metastable underwater superhydrophobicity. *Phys. Rev. Lett.* **105**, 166104 (2010).
13. D. Quéré: Wetting and roughness. *Annu. Rev. Mater. Res.* **38**, 71 (2008).
14. R.G. Karunakaran, C.-H. Lu, Z. Zhang, and S. Yang: Highly transparent superhydrophobic surfaces from the coassembly of nanoparticles (≤100 nm). *Langmuir* **27**, 4594 (2011).
15. F. Li, M. Du, Z. Zheng, Y. Song, and Q. Zheng: A facile, multifunctional, transparent, and superhydrophobic coating based on a nanoscale porous structure spontaneously assembled from branched silica nanoparticles. *Adv. Mater. Interfaces* **2**, 1500201 (2015).
16. T.-S. Wong, S.H. Kang, S.K. Tang, E.J. Smythe, B.D. Hatton, A. Grinthal, and J. Aizenberg: Bioinspired self-repairing slippery surfaces with pressure-stable omniphobicity. *Nature* **477**, 443 (2011).
17. M. Zhang, Q. Liu, R. Chen, H. Chen, D. Song, J. Liu, H. Zhang, R. Li, Y. Wang, and J. Wang: Lubricant-infused coating by double-layer ZnO on aluminium and its anti-corrosion performance. *J. Alloys Compd.* **764**, 730 (2018).
18. I. Oh, C. Keplinger, J. Cui, J. Chen, G.M. Whitesides, J. Aizenberg, and Y. Hu: Dynamically actuated liquid-infused poroelastic film with precise control over droplet dynamics. *Adv. Funct. Mater.* **28**, 1802632 (2018).
19. P. Zhang, G. Liu, D. Zhang, and H. Chen: Liquid-infused surfaces on electrosurgical instruments with exceptional antiadhesion and low-damage performances. *ACS Appl. Mater. Interfaces* **10**, 33713 (2018).
20. M. Liu, Y. Hou, J. Li, L. Tie, and Z. Guo: Transparent slippery liquid-infused nanoparticulate coatings. *Chem. Eng. J.* **337**, 462 (2018).
21. K. Rykaczewski, S. Anand, S.B. Subramanyam, and K.K. Varanasi: Mechanism of frost formation on lubricant-impregnated surfaces. *Langmuir* **29**, 5230 (2013).
22. Y. Lu, S. Sathasivam, J. Song, C.R. Crick, C. J. Carmalt, and I. P. Parkin. Robust self-cleaning surfaces that function when exposed to either air or oil. *Science* **347**, 1132 (2015).
23. C. Jia, J. Song, Y. Jin, and O.J. Rojas: Controlled-release drug carriers based hierarchical silica microtubes templated from cellulose acetate nanofibers. *J. Appl. Polym. Sci.* **132**, 38 (2015).
24. F. Ambroz, T.J. Macdonald, V. Martis, and I.P. Parkin: Evaluation of the bet theory for the characterization of meso and microporous MOFs. *Small Methods* **0**, 1800173 (2018).
25. H. Chen, P. Zhang, L. Zhang, H. Liu, Y. Jiang, D. Zhang, Z. Han, and L. Jiang: Continuous directional water transport on the peristome surface of *Nepenthes alata*. *Nature* **532**, 85 (2016).
26. Y. Wei, Z. Tian, H. Gies, R. Xu, H. Ma, R. Pei, W. Zhang, Y. Xu, L. Wang, and K. Li: Inside cover: ionothermal synthesis of an aluminophosphate molecular sieve with 20-ring pore openings. *Angew. Chem., Int. Ed.* **49**, 5200 (2010).
27. C. Ishino, M. Reyssat, E. Reyssat, K. Okumura, and D. Quere: Wicking within forests of micropillars. *Europhys. Lett.* **79**, 56005 (2007).

https://doi.org/10.1557/mrc.2018.241 Published online by Cambridge University Press